

Chem. **22**, 654 (1950).

¹²J. H. Patterson, Argonne National Laboratory Report No. ANL-5410, 1955 (unpublished).

¹³A. M. Essling, Titrimetric Determination of Uranium Using a Lead Reductor and Weight Burets, Argonne National Laboratory Analytical Group Report, 1964 (unpublished).

¹⁴When a linear trend does exist, the average of samples taken from the end of the line will tend to differ significantly from the average of samples taken from the beginning.

¹⁵A. F. Kovarik and N. I. Adams, Jr., Phys. Rev. **40**, 718 (1932).

¹⁶A. F. Kovarik and N. I. Adams, Jr., Phys. Rev. **98**, 46 (1955).

¹⁷R. Schiedt, Sitz. Akad. Wiss. Wien (Math.-naturw. Klasse), Abt. IIA **144**, 191 (1935).

¹⁸L. F. Curtiss, L. L. Stockman, and B. W. Brown, *Intercomparison of Mass Spectrometer and Alpha-Particle Methods for Isotopic Analysis*, U. S. National Bureau of Standards Report No. A-80 (U. S. GPO, Washington, D. C., 1941).

¹⁹D. E. Hull, U.S. Atomic Energy Commission Report No. MDDC-387, 1946 (unpublished).

²⁰C. A. Kienberger, Phys. Rev. **76**, 1561 (1949).

²¹R. B. Leachman and H. W. Schmitt, J. Nucl. Energy **4**, 38 (1957).

²²J. Steyn and F. W. E. Strelow, in *Metrology of Radionuclides*, edited by A. Sanielevici (International Atomic Energy Agency, Vienna, Austria, 1959), pp. 155-161.

²³The second measurement has remarkably received no notice whatsoever in review articles or summaries such as C. M. Lederer, J. M. Hollander, and I. Perlman, *Table of Isotopes* (Wiley, New York, 1967), 6th ed., p. 142. This was unfortunate, since the result reported is actually very close to our value and could have served to counterbalance the dominating high values in the intervening years.

²⁴See Lederer, Hollander, and Perlman, Ref. 23.

²⁵A. O. Nier, Phys. Rev. **55**, 150, 153 (1939).

²⁶G. Sayag, Compt. Rend. **232**, 2091 (1951).

²⁷E. Würger, K. P. Meyer, and P. Huber, Helv. Phys. Acta **30**, 157 (1957).

²⁸E. H. Fleming, Jr., A. Ghiorso, and B. B. Cunningham, Phys. Rev. **88**, 642 (1952).

²⁹G. B. Knight, Oak Ridge National Laboratory Report No. K-663, 1950 (unpublished).

³⁰A. J. Deruytter, I. G. Schroder, and J. A. Moore, Nucl. Sci. Eng. **21**, 325 (1965).

³¹P. H. White, G. J. Wall, and F. R. Pontet, J. Nucl. Energy Pt. A&B **19**, 33 (1965).

³²P. O. Banks and L. T. Silver, J. Geophys. Res. **71**, 4037 (1966).

Parity-Violating Asymmetry of the 501-keV Gamma Ray Emitted in the Decay of $^{180m}\text{Hf}^\dagger$

K. S. Krane, C. E. Olsen, James R. Sites,* and W. A. Steyert

Los Alamos Scientific Laboratory, University of California, Los Alamos, New Mexico 87544

(Received 16 June 1971)

The parity-violating forward-backward asymmetry of the 501-keV γ radiation emitted by ^{180m}Hf polarized at low temperatures is measured to be $-(1.66 \pm 0.18)\%$ at a polarization of 72%. From this asymmetry the magnitude of the irregular $E2/M2$ mixing ratio is deduced to be 0.038 ± 0.004 , in good agreement with results of circular polarization measurements. The regular $E3/M2$ multipole mixing ratio of the 501-keV γ ray is deduced to be 5.3 ± 0.3 , in agreement with results of directional-correlation measurements. The hyperfine splitting energy of ^{180m}Hf introduced as an impurity in ZrFe_2 is deduced to be $-(7.9 \pm 0.5)$ mK.

I. INTRODUCTION

The current-current theory of the weak interaction^{1,2} indicates that nuclear levels may not be states of pure parity, and that there exist small admixtures of wave functions of parity opposite to that of the strong interaction. The relative amplitude of this admixture is estimated³ to be the order of 10^{-7} the parity-conserving strong interaction, and thus the parity-violating component is expected to produce very small experimental ef-

fects. Comprehensive reviews of experiments demonstrating parity-violating effects are given by Hamilton⁴ and Henley.⁵

Considerations of nuclear-structure effects may lead to enhancement of the size of the parity-violating experimental effect. The close presence of nuclear states of opposite parity and identical spin may enhance the parity admixture in the states; the retardation of the regular parity-conserving transitions by nuclear-structure effects can often result in a larger laboratory effect. Thus in a

number of nuclei, the parity-violating effect is observed with an amplitude considerably larger than 10^{-7} .

We report here the observation of the forward-backward asymmetry in the angular distribution of the 501-keV γ radiation from polarized ^{180m}Hf samples. A preliminary report of this work has previously been published.⁶

The angular-distribution method for detecting γ -ray parity violation has certain advantages over measurements of circular polarization of radiation emitted by unpolarized sources, the method commonly used to observe parity violation in this mass region.⁴ The observation of the circular polarization of γ radiation is a relatively inefficient process, and to compensate for the small measured effects, circular polarization measurements require extremely strong radioactive sources (~ 1 Ci). Such high counting rates produce a complete degradation of detector energy resolution, and as a result the integrated γ -ray spectrum is observed, rather than individual γ rays. Since several other transitions besides the one of interest are present in the ^{180m}Hf decay, the parity-violating effect is diluted. The present work, however, employs counting rates sufficiently low for direct observation of the (relatively weak) 501-keV γ ray. Furthermore, circular polarization measurements are sensitive only to $M2$ - $\bar{E}2$ interference of the 501-keV radiation, while the angular-distribution measurements show $E3$ - $\bar{E}2$ interference as well; thus the effect measured in the present work is enhanced over that of circular polarization measurements by a factor of order $(1 + \delta)$, where δ is the $E3/M2$ mixing ratio of the 501-keV

γ ray. The net result of the ability to observe directly the 501-keV radiation with its relatively large $E3/M2$ δ is that the laboratory effect of the irregular $\bar{E}2$ parity-violating component is the order of 10^{-2} in the angular-distribution measurements as compared with 10^{-5} reported in circular polarization measurements.^{7, 8}

II. ^{180}Hf LEVEL SCHEME

The level scheme of ^{180}Hf populated by the decay of 5.5-h ^{180m}Hf is illustrated in Fig. 1. The positive-parity states are members of the $K=0$ ground-state rotational band, while the metastable 8^- state is the lowest member of the $K=8$ band. The lower multiplicities of transitions from the 8^- state to the ground-state band should thus be considerably retarded since $\Delta K=8$.

The parity-violating component of the nucleon-nucleon interaction permits a small admixture of the 8^+ level into the 8^- level, and transitions from the 8^- level may be expected to exhibit parity impurities. Measurements⁹ of the L conversion coefficients of the 57-keV transition indicated anomalous values which could be explained by the presence of a 10% irregular $\bar{M}1$ admixture into the regular $E1$ transition; however, an alternative interpretation in terms of nuclear penetration effects⁹⁻¹¹ is likewise compatible with the observed conversion coefficients. Measurement¹⁰ of the vanishing circular polarization of the 57-keV γ ray disclosed no parity impurities and thus supported the interpretation in terms of penetration effects.

The conversion coefficients^{9, 12} and circular polarization^{7, 8} of the 501-keV transition have also been measured. The conversion coefficients indicate a predominantly $E3$ multipolarity, but they are not very sensitive to irregular $\bar{E}2$ components. Michel³ has estimated that a significant $\bar{E}2$ contribution would not be expected if the regular $M2$ component were large; based on that estimate, the small magnitude of the $M2$ admixture of the 501-keV transition indicates that an observable parity-violating $\bar{E}2$ component may be present. Circular polarization measurements^{7, 8} have confirmed the presence of an irregular $\bar{E}2$ component in the 501-keV transition. As discussed above, the present experiment is more sensitive to this admixture by a factor of order $(1 + \delta)$; the $E3/M2$ mixing ratio δ of the 501-keV transition has been determined^{13, 14} by directional-correlation techniques to be $+5.5 \pm 0.1$ using the sign convention of Krane and Steffen¹⁵ for δ .

No evidence of parity violation is expected for the other transitions emitted in the decay of ^{180m}Hf , but the angular distributions of such transitions, all of which are expected to be pure $E2$, are use-

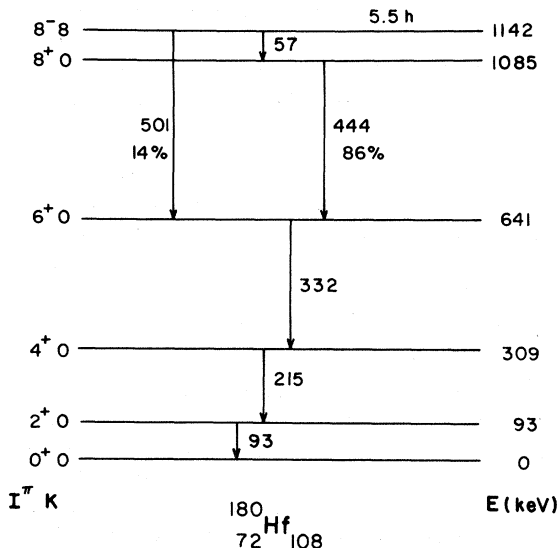


FIG. 1. Decay scheme of ^{180m}Hf .

ful for determining the polarization of the initial state.

III. EXPERIMENTAL DETAILS

A. Sample Preparation

In order to polarize the ^{180m}Hf nuclei, it is necessary to apply a large magnetic field at low temperatures. Sufficiently large hyperfine magnetic fields may be achieved at impurity sites in a ferromagnetic host lattice. Unfortunately, the alloy HfFe_2 is not cubic, and is therefore difficult to polarize in a polycrystalline sample. Instead, the alloy used was $(\text{Hf}_x\text{Zr}_{1-x})\text{Fe}_2$, prepared by arc-melting natural hafnium, zirconium, and iron. Actually, two alloys were prepared with $x=0.1$ and with $x=0.2$. The alloys were annealed at 950°C for 16 h, and then sanded to the desired shape for the experiment. X-ray analysis revealed the alloys to be of single-phase cubic structure, and they were also observed to be ferromagnetic at room temperature.

Samples 1 and 2 were obtained from separate pieces of the 10% alloy ($x=0.1$); sample 3 was cut from the 20% alloy. Sample 1 was in the form of a 6-mm-diam, 0.5-mm-thick disk; sample 2 was a pair of 0.5-mm \times 1-mm \times 6-mm "needles" oriented along the field direction for ease of polarization; sample 3 was a single 0.25-mm \times 1-mm \times 6-mm needle oriented along the field. All samples were activated in the Los Alamos Omega West Reactor, receiving total integrated fluxes of $(1-2) \times 10^{16}$ neutrons/cm². Sample 3 was annealed following the irradiation for $\frac{1}{2}$ h at 750°C ; samples 1 and 2 were placed directly in the experimental apparatus following the irradiation.

B. Apparatus

The low temperatures necessary to achieve an observable anisotropy in the angular distributions were achieved using a ^3He - ^4He dilution refrigerator, capable of continuous operation at 14 mK in the absence of a heat load. The sample was sol-

dered to a thin copper disk using Wood's metal solder; the copper disk, of approximately the same diameter as the sample, was thermally connected through a bundle of copper wires to the mixing chamber of the refrigerator. In experiments using sample 1, a source of ^{54}Mn in Fe foil was soldered to the sample; the angular distribution of the 835-keV ^{54}Mn γ ray was used to deduce the temperature.

The polarization of the alloy was achieved by a magnetic field produced by two pairs of perpendicularly oriented superconducting Helmholtz coils, illustrated schematically in Fig. 2. The current through the coils (approximately 8 A) could be manually varied so that the applied field could be made to point in any direction. The field was periodically rotated smoothly among the 0, 90, and 180° counting angles; the period for the manual field rotation was approximately 1 min.

The γ rays were detected using two stationary 40-cc Ge(Li) detectors placed on opposite sides of the source, as illustrated in Fig. 2. Each detector output was connected to a shaping amplifier and then to a multichannel analyzer.

The forward-backward asymmetry was observed by counting for fixed periods of time (10 or 20 min) with the magnetic field pointing toward one or the other of the detectors. An occasional counting period with the field at 90° relative to the detectors allowed observation of the normal equatorial-polar anisotropy of the angular distribution, for purposes of determining the degree of polarization. Since the direction of the field could be reversed, it was not necessary to compare the counting rates in the two detectors to measure the asymmetry; rather, the counting rates for a given detector were compared for the cases in which the field pointed toward or away from the detector. Such a method eliminates the need to correct for detector efficiencies, misalignment of detectors, and so forth.

C. Data Analysis

The angular distribution of γ radiation from oriented nuclear states is described by an equation of the form¹⁶

$$W(\theta) = \sum_k Q_k B_k U_k A_k P_k(\cos\theta), \quad (1)$$

where Q_k correct for the angular resolution of the detectors, B_k give the orientation of the initial state, U_k correct for depolarization due to unobserved intermediate decays, and A_k describe the properties of the observed γ ray. The P_k are the ordinary Legendre polynomials. Equation (1) is normalized such that $Q_0 = B_0 = U_0 = A_0 = P_0 = 1$. Although in most angular-distribution measure-

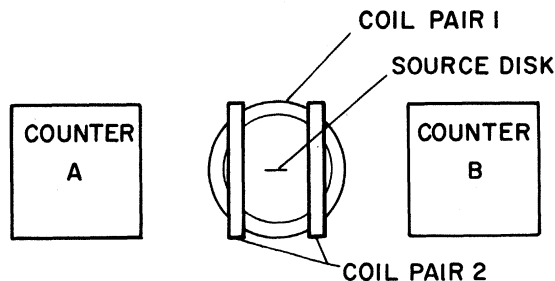


FIG. 2. Schematic of arrangement of counters, polarizing field coils, and source.

ments only even values of k are considered, the existence of parity impurities in the γ -radiation field gives rise to terms having odd values of k . The maximum value of k is determined by the spins of the nuclear states and by the γ -ray multiplicities. In the present case, for the quadrupole 444-keV transition, $k_{\max}=4$, and for the mixed quadrupole-octapole 501-keV transition, $k_{\max}=6$. Values of Q_k for Ge(Li) detectors have been computed from the geometry of the present experiment.¹⁷

The unnormalized angular-distribution coefficients A'_k are defined as^{4, 16, 18}

$$A'_k = \sum_{\substack{LL' \\ \pi\pi'}} [1 + (-1)^{\Lambda_\pi + \Lambda_{\pi'} + L + L' + k}] F_k(LL'I_f I_i) \times \langle I_f \| L\pi \| I_i \rangle \langle I_f \| L'\pi' \| I_i \rangle^*, \quad (2)$$

where the sum is carried out over the multiplicities L , L' and characters π , π' (electric or magnetic) which contribute to the radiation field. The F coefficients $F_k(LL'I_f I_i)$ are defined in Ref. 16. The parameters Λ_π and $\Lambda_{\pi'}$ are 0 for electric radiation and 1 for magnetic. For $k=\text{even}$, Eq. (2) reduces to the familiar form (neglecting parity-violating terms)

$$A_k = \frac{A'_k}{A'_0} = \frac{F_k(LL'I_f I_i) + 2\delta F_k(LL'I_f I_i) + \delta^2 F_k(L'L'I_f I_i)}{1 + \delta^2}, \quad (3)$$

where δ is the γ -ray mixing ratio for $L' = L + 1$,

$$\delta = \frac{\langle I_f \| L'\pi' \| I_i \rangle}{\langle I_f \| L\pi \| I_i \rangle}. \quad (4)$$

The irregular parity-violating components enter into the terms for even k only to second order. For odd k , we have (for the case in which only the lowest-order irregular multipole is present)

$$A_k = \frac{2\epsilon}{1 + \delta^2} [F_k(LL'I_f I_i) + \delta F_k(LL'I_f I_i)], \quad (5)$$

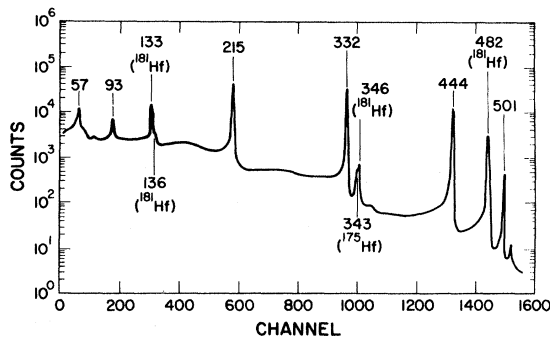


FIG. 3. γ -ray spectrum from thermal-neutron-activated $(\text{Hf}_x\text{Zr}_{1-x})\text{Fe}_2$ alloy.

where the irregular mixing ratio ϵ is defined as

$$\epsilon = \frac{\langle I_f \| L\tilde{\pi}' \| I_i \rangle}{\langle I_f \| L\pi \| I_i \rangle}. \quad (6)$$

[Terms of order ϵ^2 have been neglected in Eqs. (3) and (5).] The quantity in square brackets in Eq. (5) is the factor by which the asymmetries measured in the present work are enhanced over those measured by circular polarization.

Observation of the counting rates $W(0^\circ)$ and $W(90^\circ)$ of the pure $E2$ 444-keV transition allowed extraction of the B_2 and B_4 for the initial oriented state (assuming a pure dipole 57-keV transition), from these values of the orientation parameters, the hyperfine splitting parameter Δ/T could be deduced. Here Δ is the hyperfine energy splitting $\mu H / I k_B$ (in units of temperature) for a state of spin I and magnetic moment μ in a magnetic field H ; k_B is the Boltzmann constant. The value of Δ/T may then be used to extract the coefficients B_1 and B_3 . The sign of B_1 and B_3 is determined by the sign of Δ ; for $\Delta > 0$, B_1 and B_3 are negative.

The 0–180° asymmetry of the 501-keV transition is given by

$$\alpha = \frac{W(0^\circ) - W(180^\circ)}{\bar{W}} \cong \frac{2Q_1 B_1 A_1 + 2Q_3 B_3 A_3}{1 + Q_2 B_2 A_2 + Q_4 B_4 A_4}, \quad (7)$$

where \bar{W} is the average of the 0 and 180° counting rates. (Since there are no radiations intermediate between the oriented level and the 501-keV transition, $U_k = 1$.) Determination of the B_k from the angular distribution of the 444-keV transitions thus allows a unique determination of the irregular mixing ratio ϵ from the observed asymmetry α . In addition, observation of the 501-keV counting rate at 90° permits an independent determination of the $E3/M2$ mixing ratio δ .

The counting rates $W(\theta)$ were extracted by summing the counts in the multichannel-analyzer spectra. A typical spectrum is illustrated in Fig. 3. A linear background was assumed for the 444-keV transition, and the peak counting rates were obtained by summing the counts above that background. In the case of the 501-keV transition, it was more difficult to assign the background correction because of the presence of the 482- and 511-keV peaks in the vicinity of the 501-keV peak. Contributions to the background were mainly due to Compton-scattered events from higher-energy transitions, primarily from ^{59}Fe and ^{97}Zr activity, and to pulse pileup in the amplifier. The latter problem was alleviated somewhat by the placing of 1.5-mm lead shields in front of the detector, thus absorbing the high-intensity low-energy transitions not involved in the measurement.

Uncertainties associated with background corrections for the 501-keV line were minimized through

the use of a difference method in the data analysis. The asymmetry for a given point was computed by comparing the raw counting rates (uncorrected for background) for each point with a time logarithmic average of the two points before and after having the field in the opposite direction. The (unnormalized) asymmetry α'_i associated with point i is thus obtained from the counting rates W_{i-1} , W_i , and W_{i+1} as

$$\alpha'_i = e^{\lambda t_i} \left[W_i - \exp \left(\ln W_{i-1} + \frac{\ln W_{i+1} - \ln W_{i-1}}{t_{i+1} - t_{i-1}} (t_i - t_{i-1}) \right) \right], \quad (8)$$

where the individual asymmetries have been decay-compensated relative to an arbitrarily assigned $t=0$ ($\lambda = \text{decay constant}$).

The statistical error associated with such a difference method gives an uncertainty (also decay-compensated)

$$\Delta \alpha'_i = e^{\lambda t_i} (3W_i/2)^{1/2}. \quad (9)$$

The asymmetry for a complete measurement is obtained by computing the weighted average of the individual values of α'_i :

$$\alpha' = \frac{\sum_{i=1}^N \alpha'_i / (\Delta \alpha'_i)^2}{\sum_{i=1}^N 1 / (\Delta \alpha'_i)^2}, \quad (10)$$

$$\Delta \alpha' = \sqrt{\frac{4}{3}} \left(\sum_{i=1}^N 1 / (\Delta \alpha'_i)^2 \right)^{-1/2}. \quad (11)$$

The factor $\sqrt{\frac{4}{3}}$ in Eq. (11) is introduced in order to compensate for the fact that the errors are correlated, since each point is used twice as a nearest-neighbor point. If the data points were analyzed pairwise, rather than in groups of three, the factor in Eq. (9) would be $\sqrt{2}$ rather than $\sqrt{\frac{4}{3}}$.

A measure of the dispersion of the individual values of α'_i is given by the normalized χ^2 value:

$$\chi^2 = \frac{1}{N-1} \sum_{i=1}^N (\alpha' - \alpha'_i)^2 / (\Delta \alpha'_i)^2. \quad (12)$$

The summations of Eqs. (10)–(12) were carried out separately for the 0° and for the 180° points, i.e., separate values of α'_i , $\Delta \alpha'_i$, and χ^2 were computed for odd and even values of the summation index i . These two sets of results were then compared to arrive at a final value for the result of the measurement.

The normalized asymmetry α was obtained by dividing the unnormalized asymmetry α' by the average counting rate \bar{W} of Eq. (7) for the data point assigned to be $t=0$. Computation of \bar{W} required that the 501-keV counting rate be corrected for background effects, which was accomplished

by assuming a linear background in the vicinity of the 501-keV peak. The principal advantage of using the difference method to compute the asymmetry is that background effects cancel when the difference between successive data points is taken. Thus the background for the 501-keV peak need only be computed once for each measurement (to calculate \bar{W}), eliminating the possibility of introducing systematic errors by computing the background for each data point.

For the measurements involving source 3, a high-resolution detector and large multichannel analyzer were employed, and the improved separation of the 482-, 501-, and 511-keV γ rays made possible a point-by-point background correction to the 501-keV line. Figure 4 illustrates the counting rates corrected for background and for radioactive decay, plotted as a function of time during two half-lives of the source. Data points for which the field points away from the detector lie consis-

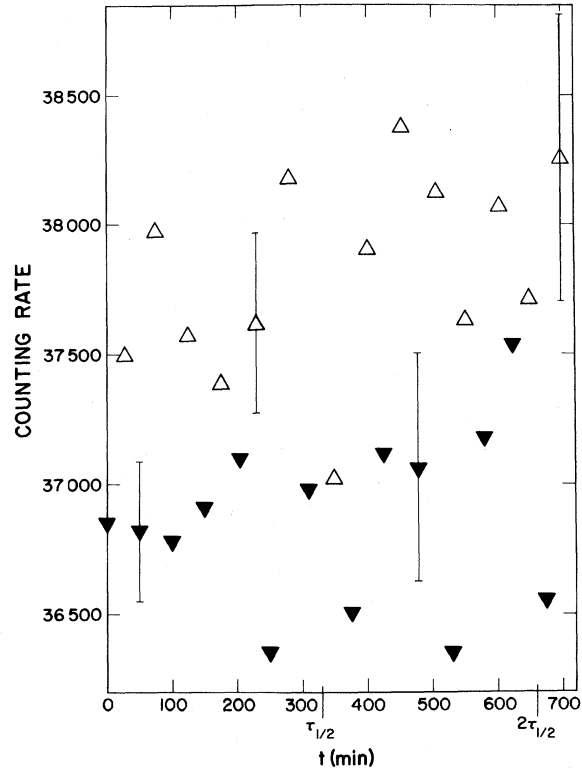


FIG. 4. Counting rate of 501-keV line as a function of time during two half-lives of measurement using $^{180\text{m}}\text{Hf}$ sample 3. The vertical axis indicates the number of counts accumulated in a 20-min counting period. Open points are those for which the field points away from the detector; filled-in points are those for which the field points toward the detector. The points have been corrected for background and for the 5.5-h decay half-life. Error bars include background uncertainty along with statistical counting uncertainty.

tently above those for which the field points toward the detector, illustrating the magnitude of the parity-violating effect. The apparent increase of counting rate with time shown in Fig. 4 is probably due to a small uncertainty in the background correction and in the half-life used to correct for the decay of the source (5.5 h). Although this method yields an unambiguous asymmetry, the quoted asymmetry values were calculated as described previously, comparing each point with the field reversed points immediately preceding and following.

IV. RESULTS

In Table I, results of the present investigation are presented for the asymmetries α of the 501-keV transition. From the equatorial-polar anisotropy of the 501-keV transition, we deduce for its $E3/M2$ mixing ratio

$$\delta(501) = +5.3 \pm 0.3, \quad (13)$$

in excellent agreement with the directional-correlation results.^{13,14} Based on the above δ , we compute from Eq. (5) $A_1 = 0.153\epsilon$ and $A_3 = -0.063\epsilon$; using the B_1 and B_3 values deduced on the basis of the 444-keV angular distribution, the values of $|\epsilon|$ can be computed from the appropriate value of α using Eq. (7). These values are tabulated in Table I. The uncertainties of the values of $|\epsilon|$ deduced from measurements of sample 1 have been increased by an arbitrary factor of $\sqrt{2}$ to allow for the possibility that the smaller field coil currents (6 A) did not fully polarize the disk-shaped source.

There is good agreement among the six individual measurements of the asymmetries, and the individual χ^2 values indicate that the dispersion of the data points was consistent with the experimental uncertainty.

There is an ambiguity in the choice of the sign of the deduced values of ϵ , due to the uncertainty in the sign of B_1 and B_3 deduced from the angular distribution of the 444-keV transition. However, the excellent agreement between the present results and those from circular polarization measurements^{7,8} clearly indicates the choice of the negative sign, and we conclude

$$\epsilon = -0.038 \pm 0.004. \quad (14)$$

The negative value of the asymmetry together with the choice of the negative sign for ϵ yield positive values for B_1 and B_3 , and thus we conclude that Δ is negative. The magnitude of Δ was deduced from measurements using sample 1. The B_k deduced from the 444-keV angular distribution yielded a value for $|\Delta|/T$ which varied from 0.36 ± 0.01 to 0.38 ± 0.01 as the sample cooled. During that same measurement the temperature (deduced from the angular distribution of the 835-keV ^{54}Mn γ ray) varied from 22 ± 0.5 to 20 ± 0.5 mK, and thus we conclude

$$\Delta = -7.9 \pm 0.5 \text{ mK}. \quad (15)$$

A confirmation of the validity of the time-logarithmic averaging process was obtained by performing such a process in cases in which no asymmetry was expected. For the 501-keV line, we have used this process to compare each point with

TABLE I. Parity-violating asymmetry and irregular $\tilde{E}2/M2$ mixing of the 501-keV γ ray of ^{180}Hf .

Sample No.	Detector	Asymmetry (%) ^a $\alpha \pm \Delta\alpha$	$\tilde{E}2/M2$ mixing ratio $ \epsilon $
1	A	-0.88 ± 0.46 $\chi^2 = 0.7$	0.020 ± 0.015
	B	-1.80 ± 0.58 $\chi^2 = 1.9$	0.041 ± 0.019
2	A	-1.47 ± 0.43 $\chi^2 = 1.3$	0.033 ± 0.010
	B	-2.31 ± 0.62 $\chi^2 = 2.7$	0.052 ± 0.015
3	A	-1.90 ± 0.34 $\chi^2 = 0.7$	0.044 ± 0.008
	B	-1.48 ± 0.42 $\chi^2 = 1.0$	0.034 ± 0.009

Average $|\epsilon| = 0.038 \pm 0.004$ ($\chi^2 = 0.7$)
 Jenschke and Bock (Ref. 7): $\epsilon = -0.041 \pm 0.007$
 Lipson, Boehm, and Vanderleeden (Ref. 8): $\epsilon = -0.033 \pm 0.009$

^a Measured relative to the applied external field.

the second-nearest preceding and succeeding points, those having the same field direction. Typical results for the asymmetries were an order of magnitude lower than those of Table I. A calculation for the 444-keV line based on the comparison of points having opposite field directions yielded the result $\alpha = (3 \pm 6) \times 10^{-4}$, with a χ^2 of 1.7, and a similar calculation on the background above the 501-keV line resulted in $\alpha = -(1.4 \pm 2.8) \times 10^{-3}$.

These results indicate that bremsstrahlung and other effects (such as source motion) which could give rise to spurious asymmetries are negligible.

As an additional test, the asymmetry of the 482-keV transition in ^{181}Ta was computed using the time-logarithmic averaging process. The asymmetry was computed to be

$$\alpha = (1.8 \pm 2.4) \times 10^{-4}. \quad (16)$$

This transition is also expected to exhibit a parity-violating effect.⁴ Based on circular polarization measurements¹⁹ the expected forward-backward asymmetry would be $\alpha = +2 \times 10^{-5}$, which is within the experimental uncertainty of the present results.

V. DISCUSSION

The nuclear Hamiltonian can be written in terms of a parity-conserving part \mathcal{H}_0 and a small parity-violating part \mathcal{H}_{PV} :

$$\mathcal{H} = \mathcal{H}_0 + \mathcal{H}_{PV}. \quad (17)$$

Assuming the parity impurities relevant to the present work to be due in large part to an admixture of the $8^+ K=0$ level into the 1142-keV 8^- level ($K=8$), the state vector of the 1142-keV level can be described by first-order-perturbation theory as

$$|1142\rangle \approx |8^-\rangle + \mathcal{G}|8^+\rangle, \quad (18)$$

where $|8^-\rangle$ and $|8^+\rangle$ are pure parity-state vectors, and \mathcal{G} is given by

$$\mathcal{G} = \frac{\langle 8^+ | \mathcal{H}_{PV} | 8^- \rangle}{E_{8^-} - E_{8^+}}. \quad (19)$$

From considerations of the probability of $\Delta K=8$ band mixing (based on estimates of lifetimes of K -forbidden γ transitions), Lawson and Segel²⁰ estimate

$$3 \times 10^{-10} \leq \mathcal{G} \leq 3 \times 10^{-13}, \quad (20)$$

using the estimate by Michel³ for the parity-mixing amplitude.

Considering only $8^+ K=0$ level, the matrix ele-

ment of the irregular $\bar{E}2$ operator is well approximated as

$$\langle 641 || \bar{E}2 || 1142 \rangle \approx \mathcal{G} \langle 6^+ || \bar{E}2 || 8^+ \rangle \approx \mathcal{G} \langle 641 || E2 || 1085 \rangle. \quad (21)$$

Using the relationship²¹ between the reduced transition probabilities within a rotational band and the value²² of $B(E2; 2^+ \rightarrow 0^+)$, we estimate

$$|\langle 641 || E2 || 1085 \rangle| = (5 \pm 0.5) \times 10^{-24} \text{ e cm}^2 \quad (22)$$

in terms of Bohr-Mottelson²³ matrix elements. From the lifetime of the 1142-keV isomeric state and from the branching ratios for transitions from that state we calculate $\tau(M2) = 8.5 \times 10^6$ sec for the lifetime associated with the $M2$ component of the 501-keV radiation, from which we compute

$$|\langle 641 || M2 || 1142 \rangle| = 2.2 \times 10^{-19} \mu_N \text{ cm} \quad (23)$$

again in terms of Bohr-Mottelson matrix elements.

From Eq. (6), using the above estimates, we compute

$$|\epsilon| \approx \mathcal{G} \frac{\langle 6^+ || E2 || 8^+ \rangle}{\langle 6^+ || M2 || 8^- \rangle} \approx (2 \pm 0.2) \times 10^9 \mathcal{G}. \quad (24)$$

From the experimental value of $|\epsilon|$, we obtain

$$\mathcal{G} = (1.9 \pm 0.3) \times 10^{-11}, \quad (25)$$

which is in agreement with the crude estimate of Eq. (20). Clearly, a better calculation of \mathcal{G} , based on considerations of various intrinsic levels and various weak-interaction Hamiltonians, is in order. It is hoped that the recent experimental results will stimulate such calculations.

The present results constitute the largest observed laboratory effect of parity mixing in nuclear states, with correspondingly one of the smallest relative uncertainties ($\sim 10\%$). It is further noteworthy that the present results were obtained in a relatively short period of measuring time. (Measurements were made on each sample for approximately two half-lives, a total of approximately 30 h for the three samples. Including sample preparation time and the time necessary to cool the apparatus to its operating temperature, each measurement lasted about 24 h.) Thus the measurement of angular distributions of γ radiation from oriented nuclei can reveal sizable laboratory effects due to parity impurities, and the study of such impurities provides a significant means of obtaining information regarding the fundamental nature of nuclear forces.

[†]Work performed under the auspices of the U. S. Atomic Energy Commission.

*Present address: Department of Physics, Colorado

State University, Fort Collins, Colorado.

¹R. P. Feynman and M. Gell-Mann, Phys. Rev. **109**, 193 (1958).

- ²M. Gell-Mann, *Rev. Mod. Phys.* **31**, 834 (1959).
³F. C. Michel, *Phys. Rev.* **133**, B329 (1964).
⁴W. D. Hamilton, *Progr. Nucl. Phys.* **10**, 1 (1969).
⁵E. M. Henley, *Ann. Rev. Nucl. Sci.* **19**, 367 (1969).
⁶K. S. Krane, C. E. Olsen, J. R. Sites, and W. A. Stey-
 ert, *Phys. Rev. Letters* **26**, 1579 (1971).
⁷B. Jenschke and P. Bock, *Phys. Letters* **31B**, 65 (1970).
⁸E. D. Lipson, F. Boehm, and J. C. Vanderleeden,
Phys. Letters **35B**, 307 (1971).
⁹G. Scharff-Goldhaber and M. McKeown, *Phys. Rev.*
158, 1105 (1967).
¹⁰H. Paul, M. McKeown, and G. Scharff-Goldhaber,
Phys. Rev. **158**, 1112 (1967).
¹¹R. Hager and E. Seltzer, *Phys. Letters* **20**, 180 (1966).
¹²V. S. Gvozdev, V. N. Grigor'ev, and Yu. V. Sergeen-
 kov, *Yadern. Fiz.* **8**, 3 (1968) [transl.: *Soviet J. Nucl.*
Phys. **8**, 1 (1969)].
¹³E. Bodenstedt, H. J. Körner, E. Gerdau, J. Radeloff,
 C. Günther, and G. Strubs, *Z. Physik* **165**, 57 (1961).
¹⁴S. D. Koički, A. H. Kukoč, M. P. Radojević, and J. M.
 Šimić, *Bilten Instituta Za Nuklearne Nauke "Boris Kidric"*
13, No. 3, 1 (1962).
¹⁵K. S. Krane and R. M. Steffen, *Phys. Rev. C* **2**, 724
 (1970).
¹⁶R. M. Steffen, Los Alamos Scientific Laboratory Re-
 port No. LA-4565-MS, 1971 (unpublished); S. R. de Groot,
 H. A. Tolhoek, and W. J. Huiskamp, in *Alpha-, Beta-,
 and Gamma-Ray Spectroscopy*, edited by K. Siegbahn
 (North-Holland, Amsterdam, 1965), 1199.
¹⁷D. C. Camp and A. L. Van Lehn, *Nucl. Instr. Methods*
76, 192 (1969). The Q_k for odd k are discussed by K. S.
 Krane, to be published.
¹⁸H. Frauenfelder and R. M. Steffen, in *Alpha-, Beta-,
 and Gamma-Ray Spectroscopy*, edited by K. Siegbahn
 (North-Holland, Amsterdam, 1965), Chap. XIX.
¹⁹J. C. Vanderleeden and F. Boehm, *Phys. Rev. C* **2**,
 748 (1970).
²⁰R. D. Lawson and R. E. Segel, *Phys. Rev. Letters* **16**,
 1006 (1966).
²¹M. A. Preston, *Physics of the Nucleus* (Addison-Wes-
 ley, Reading, Mass., 1962), p. 342.
²²O. Hansen *et al.*, *Nucl. Phys.* **25**, 634 (1961).
²³A. Bohr and B. R. Mottelson, *Nuclear Structure* (Ben-
 jamin, New York, 1969), Vol. I, p. 381.

Determination of the Charge and Mass Distribution in the Fission of $^{252}\text{Cf}^\dagger$

E. Cheifetz,* J. B. Wilhelmy, R. C. Jared, and S. G. Thompson

Lawrence Radiation Laboratory, University of California, Berkeley, California 94720

(Received 6 July 1971)

A new technique is presented for determining mass and charge distribution in fission. This method is based on obtaining the independent yields of the even-even fission products from the measured intensities of $2^+ \rightarrow 0^+$ ground-state band transitions deexciting the prompt-fission products. Transition intensities for members of ground-state bands in 36 even-even fission-product nuclei have been used to determine the centroids (Z_p) and widths (σ_Z) of the charge distribution for eight chains of fission products with constant mass and also to determine the centroids (Z_A), widths (σ_A), and yields (Y_Z) of the mass distribution for 12 chains of fission products with constant charge. The method has been applied to analyze the charge and mass distributions of ^{252}Cf spontaneous fission. The results when compared with the standard radiochemical and K x-ray technique give satisfactory agreement. The discrepancies which exist are predominantly associated with regions influenced strongly by nuclear shells. Examples are given relating the observed ground-state band transition intensities with other observed fission variables such as kinetic energy release and neutron-evaporation systematics.

I. INTRODUCTION

We present in this paper a new method which has been used to determine the independent yields of many of the fission products. The method is based upon the measurement of the intensities of the prompt transitions from the lowest 2^+ level to the 0^+ ground states in even-even fission fragments. These transitions have been identified in 36 of the highest independent-yield fission products in the spontaneous fission decay of ^{252}Cf .¹⁻³

For many years studies have been made to determine the charge distribution of products formed

in fission. Much of the information has been acquired through radiochemical isolation of specific short-lived fission isotopes from which independent and cumulative fission yields of several isotopes have been obtained (for a review of these results, see Wahl *et al.*⁴). The limiting feature in the radiochemical analysis is that the majority of the high-yield prompt-fission products have very short β -decay half-lives. This makes the isolation of these isotopes quite difficult, and in general very little is known about their properties or yields. Therefore, much of the data which have been used to interpret the charge distribution have